Chapter 50
Manipulating Photons with a Dynamic Nanocavity

Yuan-Bao Zhang, Jia-Hui Chen, Chao Li, and Jun-Fang Wu

Abstract We present a simple yet effective approach to realize a movable nanocavity based on dynamically tuning the local refractive index of a photonic crystal (PC) waveguide. Using this movable cavity, we demonstrate that it can trap, store, and transfer signal photons. The approach proposed here provides a new way for manipulating photons.

50.1 Introduction

At present, there are already many methods to form high-quality factor (Q) microcavities which can strongly confine photons in a volume in optical wavelength scale, and their implementation principles are basically achieved by partially modifying the mode gap to achieve the purpose of light confinement. These traditional high-Q microcavities are mostly realized by structure modifying like locally changing the crystal lattice [1, 2] or moving some air holes to modify the width of the line defects [3–7]. These irreversible realization methods determine that the position of their microcavities are fixed. We proposed a new method for realizing high-Q microcavities which can be formed instantly at any time and at any position in the waveguide, have a high Q, and can be moved at will. We also applicate this method to optical storage. Traditional optical storage structures based on high-Q microcavities are passive that the process of light entering the microcavity requires complex Q-switching technology (first enter when the structure is adjusted to low Q, and then store when adjusted to high Q). In addition, when these structures try to release stored signal light, the light will travel along the waveguide at both ends of the microcavity, which is said that the direction cannot be controlled. The optical storage structure we designed base on our new method of high-Q microcavity implementation is active. It can grab any part of signal light at any time during the light travel process and achieve efficient storage without Q-switching. At the same time, in the light release process,

Y.-B. Zhang · J.-H. Chen · C. Li · J.-F. Wu (✉)
School of Physics and Optoelectronic Technology, South China University of Technology, Guangzhou 510640, China
e-mail: wujf@scut.edu.cn

G. Liu and F. Cen (eds.), *Advances in Precision Instruments and Optical Engineering*, Springer Proceedings in Physics 270, https://doi.org/10.1007/978-981-16-7258-3_50

our structure can make the stored signal light transmit in the specified direction with only a simple operation other that a complex Q-switching one. In addition, unlike the traditional optical storage structure that light is trapped in a static microcavity, we can move the captured signal light to any desired position by moving the high-Q microcavity, and the moving speed can be arbitrary controlled, which is more flexible than traditional slow light waveguides [8–11].

In order to realize light storage and light release, we designed a new structure. Our structure is based on the W1 line-defect waveguide in a 2D triangular air-hole dielectric photonic crystal slab (PCS) which is shown in Fig. 50.1a. We reduce the refractive index of dielectric in the two rectangular shaded areas shown in Fig. 50.1b, while the refractive index of the air hole remains unchanged. By this way, we formed two potential barriers like what is shown in Fig. 50.1d through locally modify the mode gap so that the waveguide segment clamped by these two tuned areas, due to the presence of mirrors at both ends, forms an Fabry–Pérot (F–P) cavity. We can further understand the realization principle of forming a microcavity through two refractive index reduced regions through the calculated band structure plotted in Fig. 50.1c. Light waves that can originally propagate in the waveguide will stay in the waveguide segment clamped by the two refractive index reduced regions for the reason that the local refractive index reducing locally modified the mode gap and formed two potential barriers, therefore the light wave in the waveguide segment can exist as the resonant mode of the formed FP cavity.

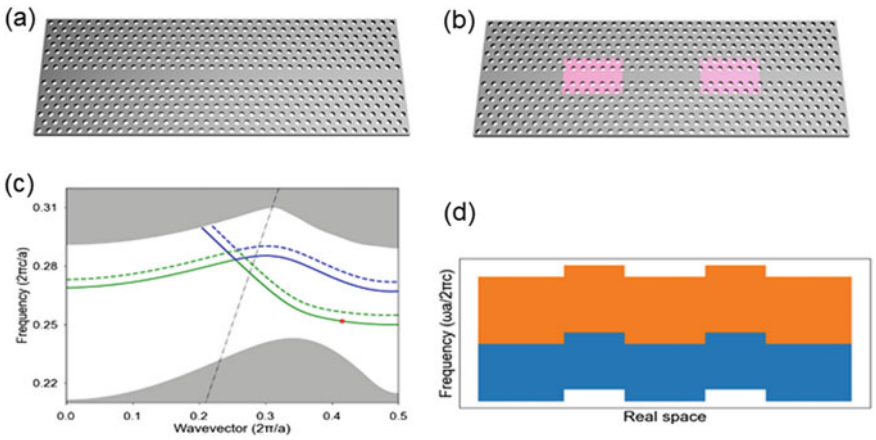

Fig. 50.1 **a** 2D triangular air-hole dielectric PC slab. **b** Refractive index tuning model structure. **c** Calculated band structure. **d** Schematic diagram along the waveguide direction

50.2 Model and Analysis

To calculate the Q and resonant wavelength of formed microcavity of our structure, we use finite-difference time-domain (FDTD) [12] to simulate our structure. The index of dielectric slab is 3.46, and the effective refractive index n used in our 2D-FDTD is 2.8. Lattice constant a, air hole radius r, and thickness t of the slab are 420 nm, 110 nm, and 210 nm respectively. For the W1 line defect used, the central distance of the nearest-neighbor air holes at both sides of line defect is $\sqrt{3}a$. The refractive index of the dielectric material in two rectangular shaded areas is $0.98n$, the length and width are 6a and 4a respectively, and the central distance of the two areas is $14a$. From the numerical calculation, we get the Q of the microcavity is 8×10^5, and the resonant wavelength is 1.67014 μm.

Compared with other mentioned methods of forming high-Q microcavities, our method does not change the structure, which means that this modulation is reversible, suggesting that we can not only stick to a static modulation approach, a dynamic one also can be used, that is, the refractive index of the dielectric material in the two shaded areas changes as a function of time, rather than constantly decreasing. We will show later that through such dynamic refractive index modulation, the structure we designed will realize the storage, release, and movement of light, which are all important parts of optical information processing.

We already know that by reducing the refractive index of dielectric material in two areas to clamp a segment of waveguide, a high-Q nanocavity can be formed between the two tuned areas. Now, we hope to make use of this, to capture light waves through dynamic tuning, and to use the formed high-Q microcavity to achieve optical storage. Figure 50.2a is the schematic diagram of our study in this section. In order to clearly see the process of a light pulse propagating and storing in our structure, we used a much longer structure in this study. The length of the structure is $87a$, and other parameters are exactly the same as the previous model structure used in Q and resonant frequency calculation. A long light pulse with a wavelength of 1.67014 μm, which is exactly the resonant frequency of the formed microcavity measured before, injected from the left end of the waveguide and propagates toward the right end. When $t = 14$ ps, the light pulse arrives the center of the waveguide, also the center of the waveguide segment clamped by these two rectangular shaded areas, the two shaded areas are modulated to decrease the refractive index of their dielectric material by 2% steeply so that their refractive index becomes $0.98n$. The Hy distribution snapshot shown in Fig. 50.2b–h shows the complete process, which begins with the injection of the light pulse and ends with storing of the light pulse. After the two shaded areas are modulated to decrease the refractive index, most of the light intensity is captured by the two modulation areas, staying at the center of the waveguide. After a long time, we can still see the light staying here. It clearly shows that we have achieved optical storage by dynamically reducing the refractive index of the two regions to clamp a segment of waveguide.

We monitored the magnetic field intensity in the center of the waveguide and plotted as in Fig. 50.3, where $t = 14$ ps is the moment we start to reduce the refractive

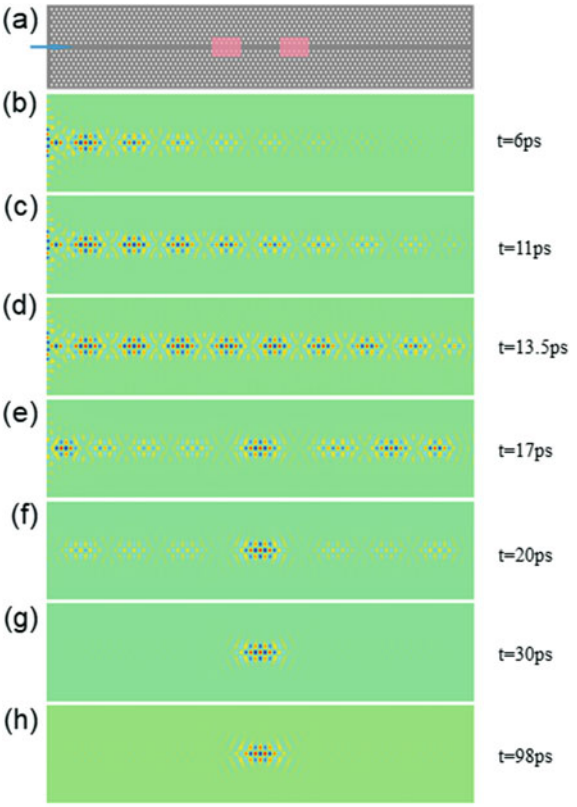

Fig. 50.2 Snapshots of field distribution in optical storage process

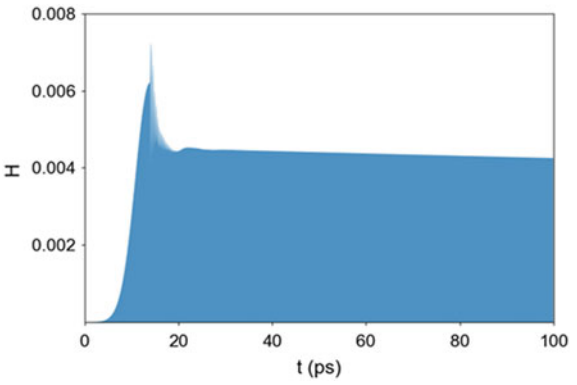

Fig. 50.3 Magnetic field in dynamic cavity as a function of time

index of the two shaded areas, which can be found in Fig. 50.3 as the moment the magnetic field intensity fluctuates sharply. It can be seen that most of the intensity of injected light is captured by the two regions and continually stay at the center of the waveguide, and for the reason that the captured light intensity exists as the resonant mode of the high-Q microcavity, its decay rate in the microcavity is very slow.

We have shown the optical storage process of our structure above. It is hard to applicate a storage structure if what been stored have not a way to be controllably released. So, in the following, we study the light release process of our structure. Continuing the optical storage process above, which we have performed dynamic modulation of the refractive index reduction on two rectangular regions at $t = 14$ ps, so that the light intensity stays between the two regions. Next, at $t = 60$ ps, we remove the refractive index modulation on the right shadow area, that is, make the refractive index of the dielectric material in the right rectangular shadow area recovers from $0.98n$ to n. Meantime, refractive index of the dielectric material in the shaded area on the left remains unrecovered and is still $0.98n$. From what have been discussed above, we already know that the light intensity can be confined between the two regions with reduction of refractive index. Then, when one of the two regions (here is the right side one) which have been reduced refractive index recover from tuning, the constraint on the light wave that originally existed on the right side of the waveguide segment will disappear so that the light wave will propagate toward the direction which the constraint is disappeared, and finally leave structure from the end of waveguide.

From the field distribution snapshots in Fig. 50.4a–e, it can be seen that the light wave that originally stored between the two tuned areas moves to the right along the waveguide after the refractive index modulation in right side shadow area is removed at $t = 60$ ps and finally leaves waveguide from the end of right side. We also monitored the magnetic field intensity at the right end of the waveguide and plot as in Fig. 50.5. It can be seen from Fig. 50.5 that there is an obvious peak at about

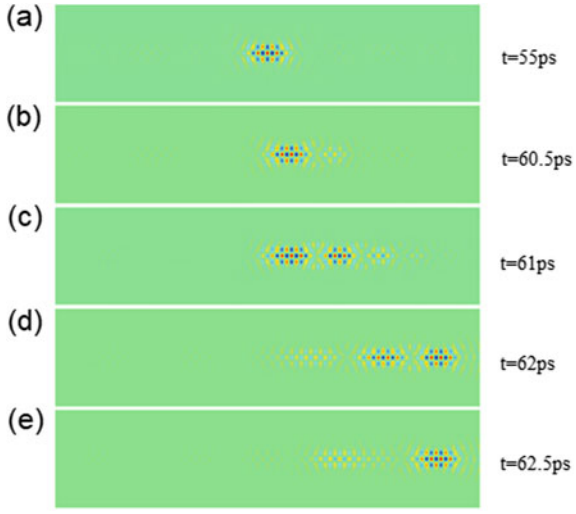

Fig. 50.4 Snapshots of field distribution in optical release process

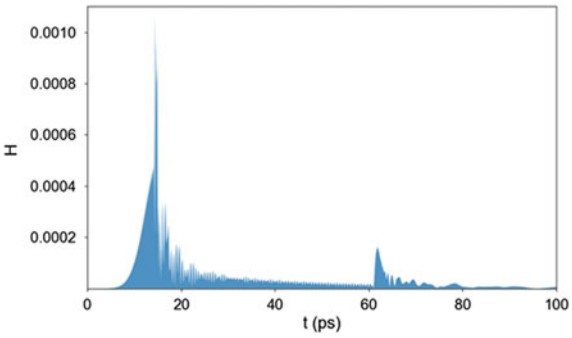

Fig. 50.5 Magnetic field at the right end of waveguide as a function of time

$t = 61.8$ ps, which is formed when the light wave leaves the right end of the waveguide after removing the modulation on the right refractive index modulated area. So far, we have realized the light release process by dynamically tuning the refractive index to remove refractive index reduction on one of two rectangular shadow areas.

Above we showed how our model structure achieve optical storage and release process through dynamical tuning. In this section, we are going to study the controllable movement of light intensity through dynamical tuning on our structure. Figure 50.6a is a schematic diagram of our study. The two dark rectangular shaded areas are the same as the previous optical storage process which will reduce their refractive index to $0.98n$ at $t = 14$ ps to complete the storage process. After the optical storage process, at a certain moment after the light intensity can stably stay between the two modulation regions, we move.

the two modulation regions toward right side which is shown by the blue arrow in Fig. 50.6a with same speed, that is, refractive index of the dielectric material in the place covered by the rectangular shaded area becomes $0.98n$, and the refractive index of the place no longer be covered recovers n. The two modulation areas finally reach and stay in the light shaded area shown in Fig. 50.6a. After the optical storage process, when $t = 40$ ps, the two refractive index reduced regions start to move to the right with a constant speed of $0.012c$. The total time of movement is 3 ps, and the final stay position for these two regions is $26a$ away from the starting position.

It can be clearly seen from the field distribution snapshots in Fig. 50.6b–f that the light intensity captured by the two refractive index reduced regions move with the movement of the two regions and finally stay between the two regions which reached the final position. And it can be seen from Fig. 50.6g that after a long time, the light intensity still stays between the two regions.

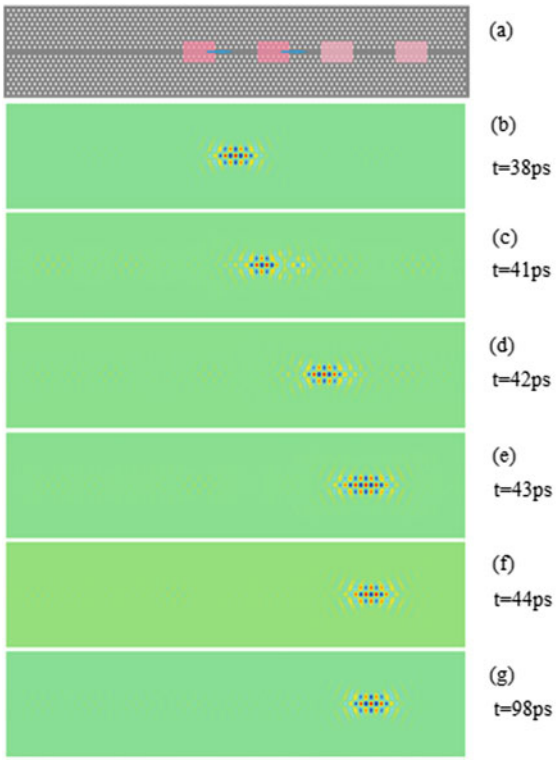

Fig. 50.6 Snapshots of field distribution in optical move process

50.3 Conclusions

In this paper, we present a simple yet effective approach to realize a movable nanocavity based on dynamically tuning the local refractive index of a photonic crystal (PC) waveguide. Using this movable cavity, we demonstrate that it can trap, store, and transfer signal photons. The approach proposed here provides a new way for manipulating photons and is promising in the fields of advanced photonic circuits, all-optical information processing, and optical communications.

Acknowledgements This research was financially supported by the National Natural Science Foundation of China (11774098); Guangdong Natural Science Foundation (2017A030313016); and Science and Technology Program of Guangzhou (202002030500).

References

1. B.-S. Song, T. Asano, S. Noda, Physical origin of the small modal volume of ultra-high-Q photonic double-heterostructure nanocavities. New J. Phys. **8**, 209 (2006)
2. B.-S. Song, S. Noda, T. Asano, Y. Akahane, Ultra-high-Q photonic double-heterostructure nanocavity. Nat. Mat. **4**, 207–210 (2005)
3. Y. Akahane, T. Asano, B.-S. Song, S. Noda, High-Q photonic nanocavity in a two-dimensional photonic crystal. Nature **425**, 944 (2003)
4. K. Ashida, M. Okano, M. Ohtsuka, M. Seki, N. Yokoyama, K. Koshino, M. Mori, T. Asano, S. Noda, Y. Takahashi, Ultrahigh-Q photonic crystal nanocavities fabricated by CMOS process technologies. Opt. Express **25**, 18165 (2017)
5. T. Asano, Y. Ochi, Y. Takahashi, K. Kishimoto, S. Noda, Photonic crystal nanocavity with a Q factor exceeding eleven million. Opt. Express **25**, 1769 (2017)
6. Y. Lai, S. Pirotta, G. Urbinati, D. Gerace, M. Minkov, V. Savona, A. Badolato, M. Galli, Genetically designed L3 photonic crystal nanocavities with measured quality factor exceeding one million. Appl. Phys. Lett. **104**, 241101 (2014)
7. Y. Akahane, T. Asano, B.-S. Song, S. Noda, Fine-tuned high-Q photonic-crystal nanocavity. Opt. Express **13**, 1202 (2005)
8. Y. Zhao, Y.N. Zhang, Q. Wang, H. Hu, Review on the optimization methods of slow light in photonic crystal waveguide. IEEE Trans. Nanotechnol. **14**, 407 (2015)
9. M.K. Moghaddam, R. Fleury, Slow light engineering in resonant photonic crystal line-defect waveguides. Opt. Express **27**, 26229 (2019)
10. S.A. Schulz, J. Upham, L. O'Faolain, R.W. Boyd, Photonic crystal slow light waveguides in a kagome lattice. Opt. Lett. **42**, 3243 (2017)
11. S. Serna, P. Colman, W. Zhang, X. Le Roux, C. Caer, L. Vivien, E. Cassan, Experimental GVD engineering in slow light slot photonic crystal waveguides. Sci. Rep. **6**, 26956 (2016)
12. A. Taflove, S.C. Hagness, *Computational Electrodynamics* (Artech House, 2000)